

# Structural and rheological evolution of silica nanoparticle gels

X. J. Cao,<sup>a</sup> H. Z. Cummins<sup>b</sup> and J. F. Morris<sup>\*a</sup>

Received 26th May 2010, Accepted 10th August 2010

DOI: 10.1039/c0sm00433b

The gelation dynamics of a sol of colloidal silica of approximately 7 nm radius particles is studied using a combination of light scattering and rheometry. By changing the ionic strength (by addition of a salt solution resulting in different ultimate molarities) of the mixture, a stable sol can be destabilized, leading to aggregation and later gelation. The gel time  $t_{gel}$  can be varied from hours to weeks, indicating a reaction-limited aggregation process. Static light scattering is used to extract the fractal dimension  $D_f$  of the aggregates, which is found to be approximately 2. The evolution of cluster size is probed by dynamic light scattering, and follows an exponential growth. Rheometry is used to assess the gelation time and further development of the network strength after gelation. The elastic modulus ( $G'$ ) is found to scale as  $G' \sim \phi^{3.3}$ , where  $\phi$  is the silica particle volume fraction. It was observed that the gel time (after salt solution addition) depends on both the particle volume fraction and salt concentration, showing a divergence at low volume fraction or low salt concentration. For a single solid fraction, data for the cluster hydrodynamic radius, normalized by the single particle radius, from experiments with a wide range of gel times can be collapsed onto a master curve when the time after the salt addition,  $t$ , is scaled as  $t/t_{gel}$ ; a similar collapse of viscosity and the linear viscoelastic data after gelation can be obtained using the same scaling of time. Salt concentration affects the gel time but not the strength of the gel network, thus allowing very accurate prediction of network formation times and mechanical properties.

## 1 Introduction

Colloidal gels are found in a wide variety of applications such as processing of ceramics, coatings, inks, personal care products, and minerals.<sup>1,2</sup> Understanding the relationship between particle interactions, the resulting gel structure and rheology is important where a particular texture or structure of gel is needed. We investigate the microstructural changes during the gelation process, and their influence on the rheological properties of the system.

The problem of gelation has been studied for a number of years. Many studies have been devoted to polymer and thermal gels to probe the characteristic gel behavior and mechanical properties of these systems.<sup>3–7</sup> While many studies have been devoted also to colloidal gels forming fractal structures, parameters controlling the behavior of the transition, the onset and nature of the stress-bearing properties of the solid-like phase, remain poorly understood. In this work, we have considered the dynamics of gelation in a colloidal silica dispersion with primary particles of  $O(10)$  nm diameter. We provide a very comprehensive study of gelation dynamics and the material properties, considering both the approach to gelation and the property evolution after gelation. Gelation is induced by adding salt to the suspending liquid, leading to screening of the silica surface charge providing a stabilizing barrier against aggregation.

The primary contributions of this work to the rather sizable literature on related systems are the determination of the gelation times by two methods, as we apply both light scattering and

rheometry, for the same system over a wide range of parameters. We demonstrate that for dilute ( $\leq 4\%$  solids by volume) dispersions, the gelation process induced by addition of salt can be scaled to master curves both before and after the gelation point using the measured gel time. The properties when presented as functions of dimensionless time are then independent of the actual rate of aggregation over orders of magnitude in this rate (or, alternatively considered, over orders of magnitude in the gel time); the properties both before the gel time (cluster size, for example) and after gelation (elastic modulus) are then functions of the particle fraction and dimensionless time only. A similar collapse, of the post-gelation properties only, was described<sup>8</sup> for gelation of a surfactant-stabilized polymer latex at somewhat higher solids fractions of  $\phi = 5–9\%$ ; in the referenced work, the scaling of time used microscopic information only and some discussion of insight resulting from a consideration of the relation between the scalings of time in our work and the Sefcik *et al.*<sup>8</sup> study is given following the presentation of our results. A practical contribution arising from this scaling is that it allows prediction of properties for conditions outside the range studied in detail.

As suggested by the comments on the contributions of this work just above, the characteristics of the colloidal suspensions can be controlled by the particle size, adjusting interparticle forces (for example, by addition of electrolyte), and the volume fraction of the dispersed phase. In an aqueous colloidal silica suspension, there is negative charge on the surface of the particles at high pH. The resulting electrostatic repulsion stabilizes the dispersion against flocculation. The ionic strength of the solution and pH control the strength of the repulsion. Addition of ions decreases both the range and the magnitude of electrostatic repulsion by reducing the Debye screening length and the zeta-potential. This screening effect of added salt leads to

<sup>a</sup>Levich Institute for Physico-Chemical Hydrodynamics and Department of Chemical Engineering, New York, NY, 10031, US. E-mail: morris@ccny.cuny.edu; Fax: +212 650 6835; Tel: +212 650 6844

<sup>b</sup>Department of Physics, City College of CUNY, New York, NY, 10031, US

destabilization of the kinetically stable system and hence to aggregation and gelation.<sup>9</sup> Change in pH alters the surface charge of silica particles, and thus destabilizes the colloidal suspension. In this paper, we focus on the effect of salt concentration and the change in solid volume fraction.

There are two limiting cases of fluid to solid transition which have been studied recently.<sup>10,11</sup> The first is for high volume fraction hard sphere particles, forming a colloidal glass characterized by trapping of particles within cages formed by nearest neighbors. The caging of the hard sphere particles leads to a colloidal glass at volume fraction  $\phi_g \approx 0.58$ . The colloidal hard sphere glass transition has been successfully studied by mode coupling theory (MCT).<sup>12–15</sup> The second limiting case is for systems with low volume fraction but strongly attractive particles. Fractal clusters are formed due to the strong interparticle interactions, finally leading to a continuous but tenuous space-filling network of colloidal gel. We study this system.

At low  $\phi$ , a scaling theory which relates the elastic properties of a gel to its network structure was developed by considering the structure of the gel network as a collection of flocs.<sup>16–19</sup> The structure of the colloidal clusters formed during the aggregation process can be described by fractal behavior, which is a simple description of the cluster geometry. It relates the mass of the cluster to its characteristic size with a single parameter, the fractal dimension  $D_f$ , which depends on the aggregation process. The fractal dimension of an object of mass  $N$  and radius  $r$  is defined by the relation<sup>16</sup>  $N \propto r^{D_f}$ . Shih *et al.* (1989) found the fractal dimension of colloidal alumina gels for dilute suspensions  $D_f \cong 1.95$  and  $D_f \cong 2.04$  from rheological measurements and static light scattering respectively.<sup>20</sup> Similarly, Lin *et al.* (1990) studied the aggregation of three different colloids (gold, silica, and polystyrene) and found the identical fractal dimension  $D_f = 2.1 \pm 0.05$  for all cases.<sup>21</sup> Later, Rueb & Zukoski (1997) studied the shear-densification effect of concentrated colloidal gels and found  $D_f = 2.5$  with preshear compared with  $D_f = 1.4$  without shear.<sup>22</sup> In addition, they demonstrated that the elastic modulus  $G'$  and the maximum strain  $\gamma_M$  in linear viscoelastic limit both scale as  $\phi/\phi_G - 1$ , where  $\phi_G$  is the gel volume fraction. Hanley *et al.* (1999) investigated the gelation of a colloidal silica system under a constant shear rate and concluded that a drop in viscosity corresponds to a structural densification.<sup>23</sup> Krall & Weitz (1997) used dynamic light scattering to measure the internal dynamics of weak fractal colloidal gels, and developed a model to determine elastic modulus which scales as  $G' \sim \phi_0^{3.9}$ , where  $\phi_0$  is the solid volume fraction.<sup>24</sup> Zackrisson *et al.* (2006) studied the effect of particle concentration and ionic strength on the irreversible colloidal silica gelation and suggested separate types of microstructure for *in situ* generation of salt and direct addition of salt solutions.<sup>2</sup> They determined the gel boundary by a prominent increase of the optical density and incipient non-ergodicity.

In this paper we present the results of a study of the aggregation kinetics of silica colloidal particles in aqueous solutions. This paper is organized in three parts. We first introduce dynamic and static light scattering and rheological methods, their basic theory and experimental set up in Part 2. Then, we discuss in Part 3 the results of dynamic and static light scattering and rheological tests performed on identically prepared samples. A short conclusion and discussion of our work follows.

## 2 Experimental methods

We used the aqueous colloidal silica suspension *LudoxSM*, pH = 10.47 (Sigma-Aldrich), consisting of amorphous silica particles with radius 7.0 nm, as reported by the manufacturer and confirmed by light scattering on diluted samples, and with 30 mass% SiO<sub>2</sub> (corresponding to a volume fraction  $\phi = 16.0\%$ ). Aggregation is initiated by the addition of aqueous NaCl (Fisher) at varying molarity under stirring. The resulting mixture was filtered across a 0.8  $\mu\text{m}$  Millipore filter for light scattering, to remove dust contamination. We will briefly outline the methods and the formulae applied in the interpretation of experiments.

### 2.1 Dynamic light scattering (DLS)

Light scattering is a method to probe the structure and dynamics of the colloidal suspension. We use it here also to determine the gelation boundary. Dynamic light scattering, which probes the size of dispersed matter, and therefore the aggregation kinetics, measures the time-averaged time correlation function of the intensity  $I(\mathbf{q}, \tau)$  of light scattered by the sample in the direction described by the scattering vector  $\mathbf{q}$ ,  $|\mathbf{q}| = (4\pi n/\lambda)\sin(\theta/2)$ ; here the refractive index of the solvent  $n = 1.33$ , wavelength  $\lambda = 488 \text{ nm}$ , and the scattering angle  $\theta = 90^\circ$ . For simplicity, we will write  $I(\tau)$  instead of  $I(\mathbf{q}, \tau)$  since  $|\mathbf{q}|$  is constant for all DLS experiments.

The normalized intensity correlation function is  $g_2(\tau)$ , described as

$$g_2(\tau) = \langle I(\tau_0)I(\tau_0 + \tau) \rangle / \langle I(\tau) \rangle^2 \quad (1)$$

For an ergodic system, the Siegert relation for the ergodic system is

$$g_2(\tau) = 1 + |g_1(\tau)|^2 \quad (2)$$

where  $g_1(\tau)$  is the normalized autocorrelation function of the scattered electric field;  $|g_1(\tau)|$  is also equal to the normalized intermediate dynamic structure factor of the sample,  $S(q, \tau)/S(q, 0)$ , where  $S(q) = \frac{1}{N} \langle \sum_i \sum_j e^{ik(\mathbf{r}_i - \mathbf{r}_j)} \rangle$  with position vectors of particles denoted  $\mathbf{r}_i$  and  $\mathbf{r}_j$ . In practice, the amplitude of the second term of (2) will be slightly reduced by the detection optics, so that

$$g_2(\tau) = 1 + a|g_1(\tau)|^2 \quad (3)$$

with  $a \leq 1$ . For a dilute suspension of spheres of hydrodynamic radius  $R_h$ ,

$$|g_1(\tau)| = \exp[-Dq^2\tau] \quad (4)$$

where  $D$  is the translational diffusion constant given by the Stokes-Einstein relation  $D = kT/6\pi\eta R_h$ . Here,  $\eta$  is the viscosity of the solvent. Eqn (4) can also be written as

$$|g_1(\tau)| = \exp[-\Gamma\tau] = \exp[-\tau/\tau_m] \quad (5)$$

where  $\Gamma = 1/\tau_m = Dq^2$ ,  $\tau_m$  is the relaxation time. Then, the normalized intensity correlation data for a dilute monodisperse colloidal dispersion can be fit directly to  $g_2(\tau) = 1 + ae^{-2(\tau/\tau_m)}$  and the radius of the colloidal particles is determined by  $1/\tau = Dq^2$ ,

with  $D \sim 1/R_h$ . For a polydisperse system, the stretched exponential function  $\exp[-2(\tau/\tau_m)^{\beta}]$  was used to obtain

$$|g_2(\tau)| = 1 + a \exp[-2(\tau/\tau_m)^{\beta}] \quad (6)$$

which can be used to fit the intensity correlation function data in order to obtain the average hydrodynamic radius  $R_h$ .

Matsunaga & Shibayama (2007) proposed several methods to determine the gel point by dynamic light scattering; one of them is “a depression of the initial amplitude of intensity correlation function (ICF)”.<sup>25</sup> We will apply this criterion to determine the gel point when the  $g_2(\tau \rightarrow 0)$  plateau drops suddenly from the value of  $g_2 \approx 2$ .

## 2.2 Static light scattering (SLS)

Static light scattering has been widely used in the study of the fractal behavior of clusters. Our SLS experiments were carried out in a BIC BI-200SM computer-controlled goniometer fitted with toluene bath. The light source is a Coherent DPSS532 532 nm diode laser. The intensity of the laser was adjusted with a variable neutral density filter to keep the intensity at the smallest scattering angle ( $15^\circ$ ) below  $2 \times 10^6$  counts per second (Mcps). Data was collected at  $5^\circ$  intervals from  $15^\circ$  to  $150^\circ$ . At each angle data was collected during three repeats of 10 s each. The intensity data was collected and converted to  $I(q)$  for  $q$  values between 0.004 and  $0.03 \text{ nm}^{-1}$ . This experiment was designed to determine the fractal dimension as well as the radius of gyration of growing silica clusters after the addition of salt to dilute silica suspensions.

If the clusters are sufficiently large,  $D_f$  can be determined directly from the angular dependence of the light-scattering intensity through a log-log plot of the static light scattering intensity  $I_{ex} = I \sin(\theta)$  vs  $q$ , which is expected to be a straight line whose slope is  $-D_f$ . The angle dependence of intensity can be fitted by the Fisher-Burford approximant,<sup>26</sup>

$$I(q) = I(0)[1 + (2/3D_f)(qR_g)^2]^{-D_f/2} \quad (7)$$

where  $R_g$  is radius of gyration. This form has the correct limiting values:

$$(qR_g) \ll 1: I(q) = I(0)[1 - 1/3(qR_g)^2] \quad (8)$$

$$(qR_g) \gg 1: I(q) = I(0)(qR_g)^{-D_f}. \quad (9)$$

## 2.3 Rheometry

Transitions of colloidal silica suspensions from liquid to gel were also monitored by rheological measurements in the linear viscoelastic regime by a strain controlled rheometer (ARES). In order to investigate the gelation transition rheologically, the samples were continuously measured after the initiation of the aggregation with Couette geometry (cup diameter: 34 mm, bob diameter: 32 mm, bob length: 33.3 mm) in oscillatory shear flow at constant frequency  $\omega = 1 \text{ Hz}$  and fixed strain 0.01. All rheological measurements were conducted at a fixed temperature of  $25^\circ \text{C}$ . In order to investigate the viscosity of the aggregating

sample, we conducted steady shear rate measurements with low shear rate  $\dot{\gamma} = 0.01 \text{ s}^{-1}$  in the same Couette geometry at temperature  $25^\circ \text{C}$ .

A classical definition of gel point (GP)<sup>27</sup> is when the steady-shear viscosity diverges to infinity, and the equilibrium modulus starts to rise, *i.e.*  $\eta_0 \rightarrow \infty, G_\infty = 0$ . However, since they involve limiting properties, GP can only be determined by extrapolation from this definition.

Another method to probe the gel transition is performed by a dynamic rheological test. The storage modulus  $G'$  and loss modulus  $G''$  obtained from the test have the same power law dependence on strain frequency at the gel point,<sup>22,28</sup>

$$G'(\omega) \sim G''(\omega) \sim \omega^m. \quad (10)$$

This is the Winter & Chambon (1987) criterion for gelation.<sup>29</sup> Here, the determination of the gel point comes from the crossover of storage and loss modulus ( $G'$  and  $G''$ ) after which  $G'$  increases more quickly than  $G''$  consistent with Drabarek *et al.* (2002)<sup>30</sup> and Matsunaga & Shibayama (2007).<sup>25</sup> It is confirmed in these studies that the crossover time is approximately equal to the gel time. Rheological determination of the gelation boundary thus rests on our ability to measure the onset of an elastic modulus; this can be quite difficult if the elastic modulus is very low, as is the case for the very tenuous solid networks. The minimum torque we can evaluate in the rheometer is approximately  $1.9 \times 10^{-6} \text{ Nm}$  with a minimum value of  $G' \approx 3.6 \text{ Pa}$ .

## 3 Results

Without salt addition, the colloidal silica suspension is stable. Repulsive forces due to the surface charge maintain particles in a non-aggregating state. Salt addition destabilizes the system by screening the Coulomb repulsion and brings the onset of aggregation and later gelation. The kinetics and mechanical properties of the gel at any time following the salt addition depend on both the salt concentration and particle volume fraction; kinetics and mechanical properties are monitored by light scattering and rheometry.

### 3.1 Dynamic light scattering

Fig. 1 shows typical intensity correlation data,  $g_2(\tau)$  from DLS after the addition of the salt solution ( $\phi = 2\%$ ,  $[\text{NaCl}] = 0.454 \text{ M}$ ). Data was collected at time intervals of 15 min. Note that  $g_2(\tau)$  decays at all relaxation times  $\tau_m$  below the gel time  $t_{gel}$ , determined by the sudden decrease of the  $g_2(\tau \rightarrow 0)$  plateau (indicated by the arrow in the figure). In addition, the relaxation times gradually increase during the gelation process; and the measured relaxation times appear to diverge as the time goes beyond about 80 min, as shown in Fig. 2. The drop of the plateau of  $g_2(\tau)$  to a much lower level indicates a reduced mobility due to long-ranged network formation. Another consequence from a rheological perspective is that the system starts to have a finite shear modulus or rigidity. Particles can move by Brownian motion, but those which are physically bonded into the network cannot move far. If they do not move at all then their correlation function is time independent and finite, which contributes to the static part of the correlation function. If they move slightly then

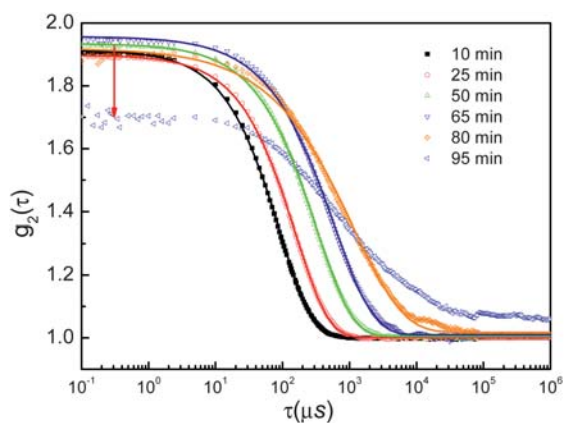


**Fig. 1** Intensity correlation functions  $g_2(\tau)$  during the gelation process ( $\phi = 2\%$ ,  $[\text{NaCl}] = 0.454 \text{ M}$ ; dot: original data; line: fitting to  $g_2(\tau) = b + a \exp[-2(\tau/\tau_m)^\beta]$ ).

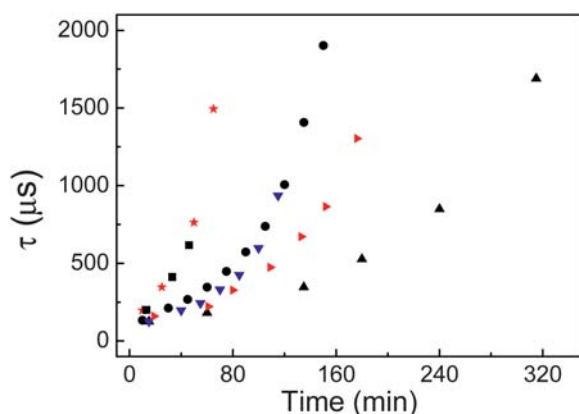


**Fig. 2** Relaxation time  $\tau$  during gelation process.  $\blacksquare$ ,  $\phi = 1.0\%$ ,  $[\text{NaCl}] = 0.548 \text{ M}$ ;  $\bullet$ ,  $\phi = 1.0\%$ ,  $[\text{NaCl}] = 0.497 \text{ M}$ ;  $\blacktriangle$ ,  $\phi = 1.0\%$ ,  $[\text{NaCl}] = 0.454 \text{ M}$ . Red  $\star$ ,  $\phi = 2.0\%$ ,  $[\text{NaCl}] = 0.454 \text{ M}$ ; Red  $\blacktriangleright$ ,  $\phi = 2.0\%$ ,  $[\text{NaCl}] = 0.398 \text{ M}$ ; Blue  $\blacktriangledown$ ,  $\phi = 4.0\%$ ,  $[\text{NaCl}] = 0.348 \text{ M}$ .

the ensemble-averaged correlation function decays to a nonzero value at long times.<sup>3</sup>

The average hydrodynamic radius of the clusters is calculated through the intensity correlation function fitted as  $g_2(\tau) = b + a \exp[-2(\tau/\tau_m)^\beta]$  and  $\langle R_h \rangle = \tau_m \frac{k_B T}{6\pi \eta} \cdot \frac{1}{\beta}$ .  $a$ ,  $b$ ,  $\tau_m$ , and  $\beta$  are determined by fitting the experimental data using a least-squares algorithm. The viscosity of water is used, which is correct for dilute  $\phi$  in the early aggregation as confirmed by viscosity measurement (Ubbelohde viscometer).

The system shows an exponential decay at the early stage of the aggregation process, with  $\beta$  equal to 1; approaching the gel point, the correlation functions progressively deviate from the exponential decay, with a continuous decrease in  $\beta$ , which is an indication of polydispersity. The size of the clusters increases rapidly with the time as shown in Fig. 3. Approaching the gel point, the average cluster size appears to diverges (though it does not) as the system forms a space-filling network. For all three cases, the initial aggregation rate is relatively slow and the rate increases as the size of the cluster increases, as large clusters have more possibilities to connect to particles and clusters.<sup>21</sup> Upon such observation, we present a simple aggregation kinetics model

that the aggregation rate  $dN/dt$  is proportional to  $R(t)^\alpha$ , where  $N$  is average number of particles in an aggregate, and  $R(t)$  is the linear size of the aggregate. As mentioned in the introduction,  $N \propto R^{D_f}$ , so that this simple model can be expressed as

$$dN/dt = k_r R(t)^\alpha = k_r N^{\alpha/D_f} \quad (11)$$

where  $k_r$  is the rate of aggregation with units of  $\text{min}^{-1}$  for the systems we studied. For reaction-limited aggregation system (RLA), we treat  $\alpha/D_f$  as unity; then  $N = N_0 \exp(k_r t)$  and  $R(t) = R_0 \exp(k_r t/D_f)$ . In Fig. 3, we show the average radius of clusters as a function of time for different salt and solid systems. The solid curves represent fittings to the exponential growth of aggregates (RLA). The aggregation constant depends on both the salt and silica concentration. The coefficient  $R_0$  and  $k_r$  are treated as adjustable parameters in the fit; while  $D_f$  is kept as a constant 2, an average number of fractal dimension as indicated by the static light scattering results in Table 2. The fitting parameters are shown in Table 1.  $R_0$  is the size of initial cluster at  $t = 0$  immediately after the salt addition. For the same silica volume fraction, the rate of aggregation ( $k_r$ ) is much faster for samples with high salt concentration and leads to more rapid gelation, in agreement with the rheological evaluation, discussed in § 3.4.

When the aggregation time  $t$  is scaled by the measured gel time  $t_{gel}$  and  $R(t)$  is scaled by the particle radius estimated as  $R_h(0)$ , the normalized average hydrodynamic radius of clusters,  $R_h(t)/R_h(0)$ , collapses into a master curve and shows an exponential

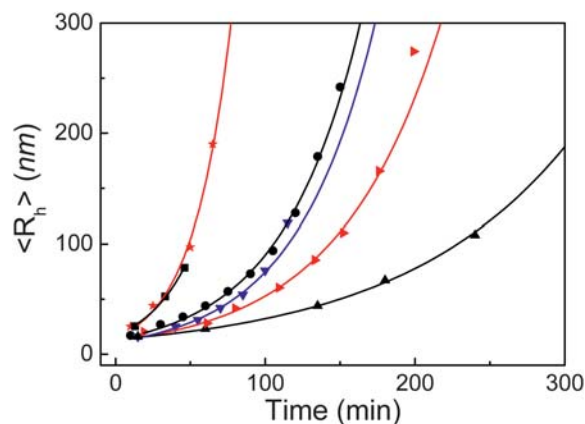


**Fig. 3** The growth of average hydrodynamic radius of clusters for samples  $\blacksquare$ ,  $\phi = 1.0\%$ ,  $[\text{NaCl}] = 0.548 \text{ M}$ ;  $\bullet$ ,  $\phi = 1.0\%$ ,  $[\text{NaCl}] = 0.497 \text{ M}$ ;  $\blacktriangle$ ,  $\phi = 1.0\%$ ,  $[\text{NaCl}] = 0.454 \text{ M}$ . Red  $\star$ ,  $\phi = 2.0\%$ ,  $[\text{NaCl}] = 0.454 \text{ M}$ ; Red  $\blacktriangleright$ ,  $\phi = 2.0\%$ ,  $[\text{NaCl}] = 0.398 \text{ M}$ ; Blue  $\blacktriangledown$ ,  $\phi = 4.0\%$ ,  $[\text{NaCl}] = 0.348 \text{ M}$ ; solid curves are exponential fittings to  $R(t) = R_0 \exp(k_r t/D_f)$ .

**Table 1** Parameters of aggregation kinetics ( $R(t) = R_0 \exp(k_r t/D_f)$ ) for volume fraction 1%–4% at different salt concentrations

$\phi$	$[\text{NaCl}]/\text{M}$	$R_0/\text{nm}$	$k_r$
1%	0.454	$14.8 \pm 2.70$	$0.018 \pm 0.0001$
1%	0.497	$12.7 \pm 0.71$	$0.039 \pm 0.0004$
1%	0.548	$17.0 \pm 1.24$	$0.067 \pm 0.0018$
2%	0.398	$12.1 \pm 0.91$	$0.030 \pm 0.0005$
2%	0.454	$14.8 \pm 2.70$	$0.078 \pm 0.0030$
4%	0.348	$6.8 \pm 1.52$	$0.048 \pm 0.0014$

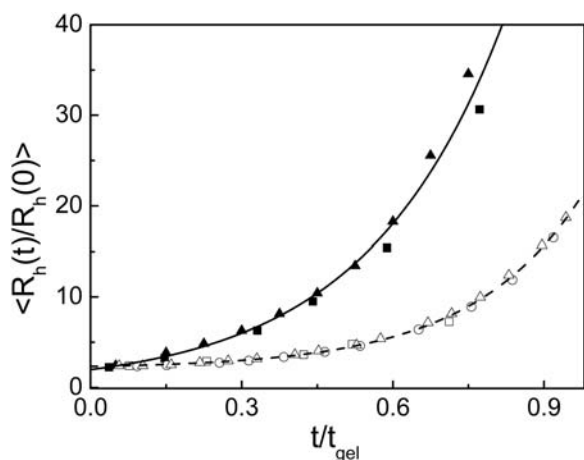


**Fig. 4** The scaled average hydrodynamic radius of clusters.  $\blacksquare$ ,  $\phi = 1.0\%$ ,  $[\text{NaCl}] = 0.497 \text{ M}$ ;  $\blacktriangle$ ,  $\phi = 1.0\%$ ,  $[\text{NaCl}] = 0.454 \text{ M}$ ;  $\square$ ,  $\phi = 5.0\%$ ,  $[\text{NaCl}] = 0.38 \text{ M}$ ;  $\circ$ ,  $\phi = 5.0\%$ ,  $[\text{NaCl}] = 0.37 \text{ M}$ ;  $\triangle$ ,  $\phi = 5.0\%$ ,  $[\text{NaCl}] = 0.35 \text{ M}$  (Lines are exponential fittings).

growth as a function of  $t/t_{gel}$  for the same silica volume fraction (Fig. 4). Hence, as a function of  $t/t_{gel}$ , the growth of cluster size is independent of the salt concentration and depends on the silica volume fraction only.

### 3.2 Static light scattering

The structure of the aggregates was investigated by the application of static light scattering. Fig. 5 shows the evolution of the scattered light intensity as a function of the scattering vector  $q$  at low volume fraction  $\phi = 0.1\%$ . At early aggregation time (0–23 min), the intensity is low and is independent of the scattering angle. As the clusters grow larger, the intensity increases and shows variation with angle. The intensity gradually grows and shows significant angular dependence until it approximates a straight line in  $\ln(I \sin \theta)$  vs.  $\ln q$ , shown in Fig. 5. The amplitude of intensity changes very little when very large clusters form. A better observation can be found in Fig. 6 for times longer than 117 h. We obtain the fractal dimension  $D_f$  and the radius of gyration  $R_g$  by fitting the intensity data by the Fisher-Burford method for both  $\phi = 1\%$  and  $\phi = 0.1\%$ , as shown in Table 2 and

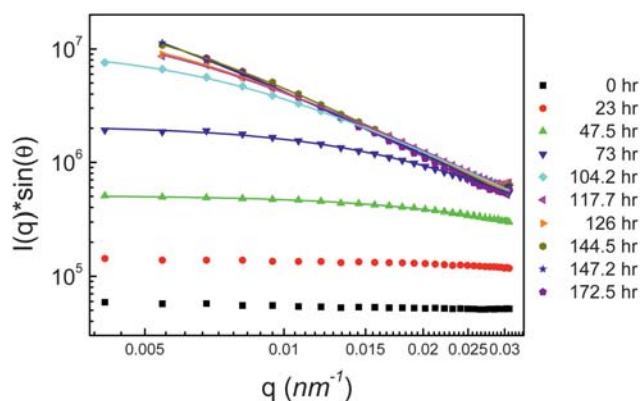


**Fig. 5** The angular dependence of intensity during the gelation process  $\phi = 0.1\%$ ,  $[\text{NaCl}] = 0.51 \text{ M}$  (Dots are experimental results; Lines are Fisher-Burford fittings).

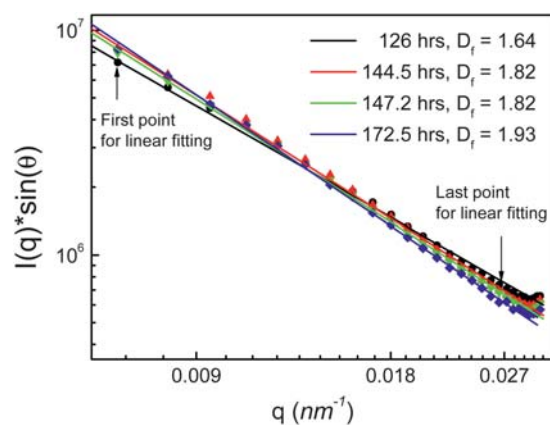


**Fig. 6** Determination of the fractal dimension during the gelation process  $\phi = 0.1\%$ ,  $[\text{NaCl}] = 0.51 \text{ M}$  (Dots are experimental results; Lines are linear fittings).

**Table 2** The fractal dimension  $D_f$  and radius of gyration  $R_g$  during gelation process obtained by Fisher-Burford method compared with hydrodynamic radius  $R_h$  ( $\phi = 1\%$ ,  $[\text{NaCl}] = 0.454 \text{ M}$ )

Time/min	$D_f$	$R_g/\text{nm}$	$R_h/\text{nm}$
140	$2.10 \pm 0.05$	$45.0 \pm 0.11$	44
185	$2.02 \pm 0.07$	$68.8 \pm 0.14$	67
245	$2.00 \pm 0.05$	$85.0 \pm 0.84$	108
320	$2.04 \pm 0.01$	$94.0 \pm 0.14$	215

Fig. 6, respectively. For systems with volume fraction  $\phi = 1\%$ , they form physically visible gels, which means the systems will not flow after being upside-down. We did not observe physically visible gels for systems with  $\phi \leq 0.75\%$ . As mentioned by Lin *et al.*,<sup>21</sup> the critical volume fraction  $\phi_0$  to complete gelation is  $\phi_0 \approx 10^{-5}$ . The radius of gyration ( $R_g$ ) is defined by the expression given below,

$$R_g^2 = \frac{\sum m_i r_i^2}{m_i r_i}, \quad (12)$$

where  $m_i$  is the mass of the  $i^{\text{th}}$  particle in the cluster and  $r_i$  is the distance from the center of mass to the  $i^{\text{th}}$  particle. The

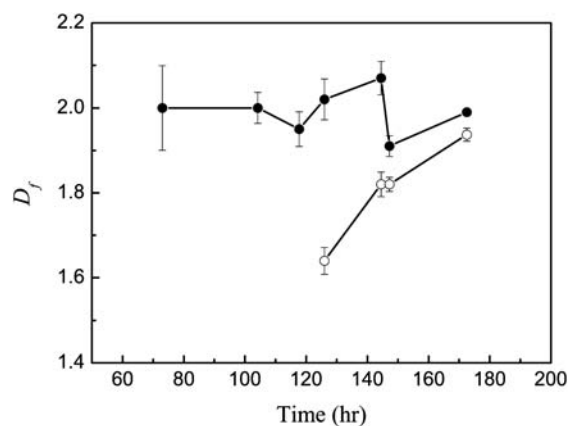


**Fig. 7** The fractal dimension  $D_f$  during the gelation process ( $\phi = 0.1\%$ ,  $[\text{NaCl}] = 0.51 \text{ M}$ ).  $\bullet$ , obtained by Fisher-Burford fitting;  $\circ$ , calculated by linear fitting.

hydrodynamic radius, as introduced in § 2.1, is calculated from the diffusional properties of the particle cluster and is indicative of the apparent size of the dynamic hydrated/solvated cluster. The comparison of  $R_g$  and  $R_h$  in Table 2 shows that they agree with each other at earlier time; approaching to the gel point, the size of the hydrodynamic radius is larger than the radius of gyration, which indicates that the system starts to form fractal objects. The fractal dimension from the Fisher-Burford method is slightly higher than that obtained from the linear fitting method, as indicated in Fig. 7. However, the results from the latter method also depend on the selection of the data points for linear fitting (Fig. 6).

### 3.3 Rheological results

Transition of aqueous silica suspensions from liquid-like to solid-like state was examined by rheological methods. We determine the dependence of the linear viscoelastic properties as a function of time for systems of various particle volume fractions and salt concentrations. The linear visco-elastic regime is determined by strain sweep measurement, in which an increasing strain is applied to the formed gel. A maximum strain  $\gamma_m$  was obtained by the response of the storage and loss modulus ( $G'$  and  $G''$ ) to the applied strain. For the gels we studied here,  $\gamma_m$  is between 10%–15%, determined by the point where  $G'$  and  $G''$  starts to have 10% deviation from the plateau level of  $G'$  and  $G''$  of small strains.

**3.3.1 Gel times.** In Fig. 8, the gel time determined rheologically is shown as a function of salt concentration for several volume fractions ( $\phi = 1\% - 4.7\%$ ). As we decrease the concentration of the salt, the gel time increases rapidly and tends to diverge at low salt concentration, consistent with stability (*i.e.*  $t_{gel} \rightarrow \infty$ ) of the as-received (no added salt) dispersion. Larger salt concentration induces a shorter time to GP, due to the stronger screening effect. The effect of silica concentration on the aggregation kinetics can also be observed in this figure. Samples with relatively low silica volume fraction evolve slowly and take more time to form space-filling gel networks, indicated by the arrow in

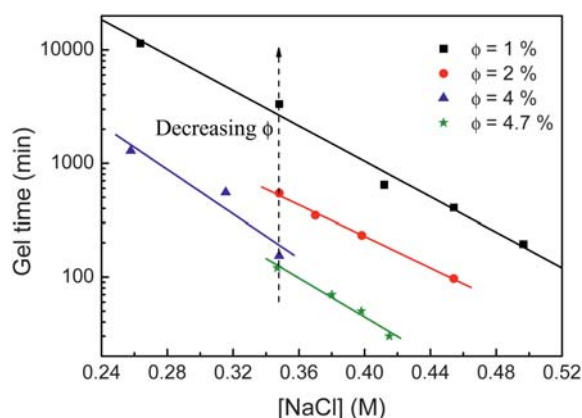


**Fig. 8** Gel time determined rheologically as a function of salt concentration for several volume fractions ( $\phi = 1\% - 4.7\%$ ); lines are given by data fitting to equation  $t_{gel} = A \exp(-\kappa[NaCl])$ , with  $\kappa = 7.8, 6.9, 9.7, 8.6$  for  $\phi = 1, 2, 4, 4.7\%$ . The arrow in the figure indicates the growth in gel time as function of  $\phi$  for the same salt concentration  $[NaCl] = 0.348$  M.

Fig. 8 at salt concentration 0.348 M. The gel time can be fitted into equation  $t_{gel} = A \exp(-\kappa[NaCl])$ , with  $\kappa = 8.3 \pm 1.2$  for  $\phi = 1\% - 4.7\%$ , and showing no clear trend of variation.

### 3.3.2 Effect of salt concentration on kinetics and gel structure.

Keeping the volume fraction of silica particles fixed at 1%, storage ( $G'$ ) and loss ( $G''$ ) modulus were measured as a function of time following salt addition at different molarities at fixed frequency 1.0 Hz and constant strain 0.01. The results are shown in Fig. 9.

For all samples,  $G'$  and  $G''$  increase with time after the network formation during the gelation process. The addition of salt solution leads to compression of the electrical double layer around each particle, and eventually to particle aggregation; the connected particles form large aggregates and finally a connected network fills the whole volume, leading to arrest. Phenomenologically, the system exhibits a “gel state”. At the same time,  $G'$  and  $G''$  become measurable in a rheological test. We determine the crossover time (when  $G'$  becomes larger than  $G''$ ) as the gel time ( $t_{gel}$ , indicated by the dashed lines in Fig. 9). After the GP, dynamics are largely due to the unconnected particles and loose particle clusters among the network, which continue to make contributions to the stiffness of the system as they attach to the space-filling network (increasing  $G'$ ). Growth in  $G'$  and  $G''$  becomes progressively slower.

It is shown in Fig. 9 that, for fixed  $\phi$ , the salt concentration affects the time at which the system forms a space-filling network. The suspension with highest salt concentration ( $[NaCl] = 0.497$  M) gels at the earliest time ( $t_{gel} = 195$  min). When the aggregation time is scaled by the gel time,  $G'$  collapses into a single master curve for the same silica volume fraction but with various salt concentrations, as shown in Fig. 10. This result indicates that during the gelation process, the three samples of the same  $\phi$  and different  $[NaCl]$  have similar mechanical strength at the scaled time, which can be further extended to argue that the gel under the same silica volume fraction has similar structure at this scaled time,  $t/t_{gel}$ . When combined with the results in DLS (as shown in Fig. 11), both the hydrodynamic radius  $R_h$  and

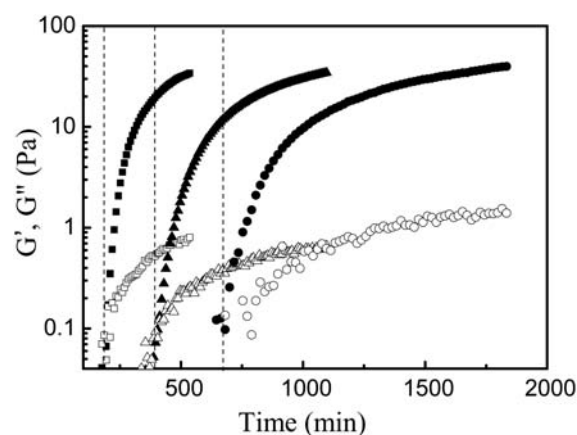


**Fig. 9** The evolution of storage ( $G'$ , solid) and loss modulus ( $G''$ , open) of samples with low silica volume fraction ( $\phi = 1\%$ ). ■, □ ( $[NaCl] = 0.497$  M,  $t_{gel} = 195$  min); ▲, △ ( $[NaCl] = 0.454$  M,  $t_{gel} = 407$  min); ●, ○ ( $[NaCl] = 0.412$  M,  $t_{gel} = 645$  min). Frequency, 1 Hz; Strain, 1%. The dash lines indicate the gel time.

storage modulus  $G'$  can be scaled by the gel time  $t_{gel}$  and collapse into two separate master curves. From the scaling behavior of different systems, we suggest there is a universal behavior in aggregation kinetics which can be related to the gel time. For the

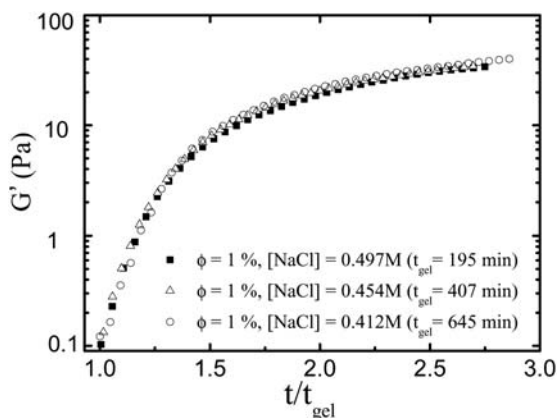


**Fig. 10** The scaling behavior of the storage modulus  $G'$  for samples with same silica volume fraction  $\phi = 1.0\%$  but various salt concentrations when time is scaled by gel time  $t_{gel}$ .

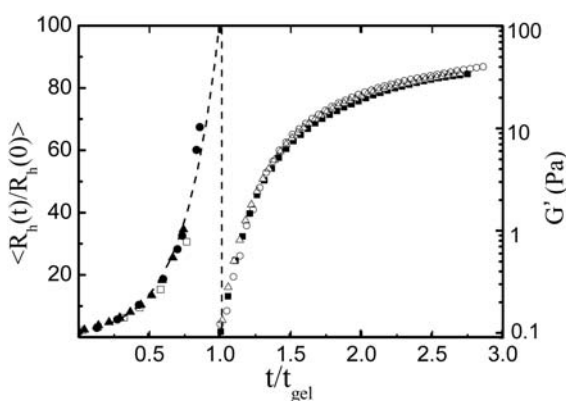


**Fig. 11** Combination of the growth of hydrodynamic radius  $R_h$  and storage modulus  $G'$  as function of time for samples with silica volume fraction  $\phi = 1.0\%$  and varies salt concentration. The left dashed line is exponential fitting to  $R_h$ ; the other line indicates the gel time.

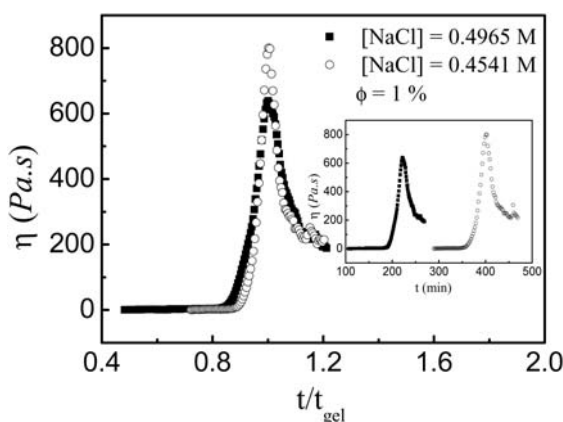


**Fig. 12** The change in viscosity,  $\eta$ , during gelation process at a shear rate of  $\dot{\gamma} = 0.01 \text{ s}^{-1}$  (■,  $\phi = 1.0\%$ ,  $[\text{NaCl}] = 0.4965$ ; ○,  $\phi = 1.0\%$ ,  $[\text{NaCl}] = 0.4541 \text{ M}$ ).

RLA process leading to the gels studied here, salt concentration only affects the aggregation rate but not the microstructure. The parameter that determines the microstructure and the strength of gel network is the silica volume fraction  $\phi$ .

The inset of Fig. 12 shows the viscosity change during the gelation process under weak shearing of  $\dot{\gamma} = 0.01 \text{ s}^{-1}$ . Upon mixing, the viscosity of the system is low and close to the viscosity of the solvent (water). Approaching the critical time, the viscosity increases until it reaches a peak value; and then it decreases rapidly. As predicted by Jansen *et al.* (1986) the suspension gels after this point, the gel time.<sup>31</sup> The rapid increase in viscosity is due to the formation of large clusters and newly-formed particle network; and the decrease in viscosity is due to the break-up of the newly-formed weak network, which then does not reform under the flow. When the time is scaled by  $t/t_{gel}$ , the viscosity also collapses into a master curve (Fig. 12). This scaling behavior is consistent with the one found in the growth of hydrodynamics radius and storage modulus of gel network. We note that there is some difference in the peak viscosities, but this is not systematic.

**3.3.3 Effect of silica concentration on kinetics and gel structure.** Above, we showed that only silica volume fraction,  $\phi$ , plays a significant role in both the structure and ultimate mechanical properties of the gels. The influence of  $\phi$  on the gel formation is illustrated in Fig. 13, in which we present the storage modulus  $G'$  and loss modulus  $G''$  at constant salt concentration ( $[\text{NaCl}] = 0.454 \text{ M}$ ) and frequency (1 Hz) for  $\phi = 1\%$  and  $\phi = 2\%$ . The increase in  $G'$  and  $G''$  is quite similar to the case seen above. Here, we see that the particles aggregate faster in the higher- $\phi$  sample: the gel time for  $\phi = 2\%$  is roughly 1/4 the value of the more dilute  $\phi = 1\%$  ( $t_{gel} = 97 \text{ min}$  and  $t_{gel} = 407 \text{ min}$  respectively). The gel with high silica volume fraction ( $\phi = 2\%$ ) builds a stronger network, with  $G'$  almost 10 times larger than the one with  $\phi = 1\%$ , roughly consistent with  $G' \sim \phi^{3.3}$ . For higher  $\phi$ , particles are in closer proximity, giving rise to a shorter gel time. In addition, there are more particles in a unit volume for higher  $\phi$ , making contributions to the gel network; as a result, the system displays a stronger network, and hence higher value of  $G'$ .

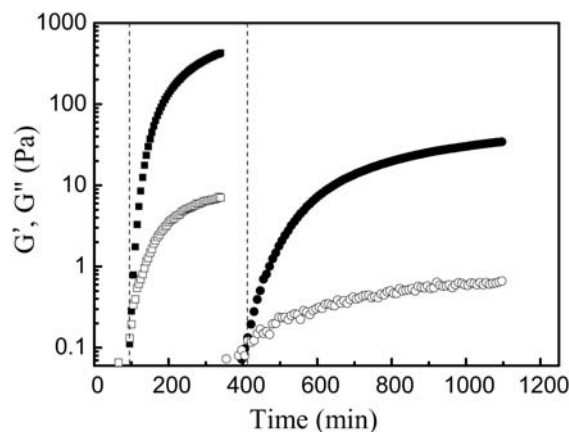


**Fig. 13** The growth of  $G'$  (solid) and  $G''$  (open) as function of time for samples with the same salt concentration  $[\text{NaCl}] = 0.454 \text{ M}$  (■, □,  $\phi = 2.0\%$ ,  $t_{gel} = 97 \text{ min}$ ; ●, ○,  $\phi = 1.0\%$ ,  $t_{gel} = 407 \text{ min}$ ). The dash lines indicate the gel time.

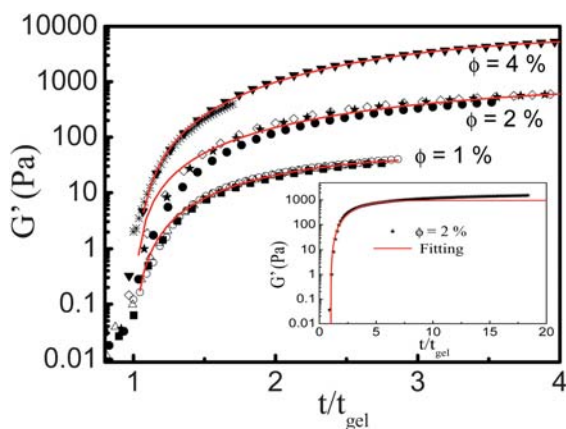


**Fig. 14** The scaling behavior of the storage modulus  $G'$  for samples with silica volume fraction  $\phi = 1.0 - 4.0\%$  when time is scaled by  $t/t_{gel}$ . Dots: experimental data; solid red lines: fittings to equation  $G' = G'_{\infty}(1 - \exp[-\alpha(t/t_{gel} - 1)^{\beta}])$ . For  $\phi = 1, 2, 4\%$ , respectively,  $G'_{\infty} = 49.1, 954.2, 6700.7$  Pa;  $\alpha = 0.55, 0.17, 0.16$ ;  $\beta = 1.64, 1.61, 2.07$ .

Fig. 14 shows that the scaling behavior of  $t/t_{gel}$  collapses the  $G'$  data for  $1\% \leq \phi \leq 4\%$ , showing again that the salt concentration only effects the gel time not the strength of the particle network at the scaled time. Rueb & Zukoski (1997) used a first-order model<sup>22</sup> to describe the growth of  $G'$ . Based on their model, we propose a similar model,

$$G' = G'_{\infty}(1 - \exp[-\alpha(t/t_{gel} - 1)^{\beta}]) \quad (13)$$

where  $\alpha$  is the rate of increase of  $G'$ , which is a measure of the rate of increase in structure or the degree of connectedness within the gel;  $\beta$  is a stretched exponential coefficient (due to low solid volume fraction compared with Rueb's dense systems). The red solid curves show the results of fitting the experimental data to the above model within a scaled time  $1 \leq t/t_{gel} \leq 4$ . The model matches the data well in the scaled time range. The inset of Fig. 14 shows the growth of storage modulus of system with volume fraction  $\phi = 2\%$  for larger time range, in order to check the prediction of this fit. As shown in the inset, the model works well to the scaled time  $t/t_{gel} = 10$ , after which, the prediction saturates more rapidly than the experimental  $G'$ , which continues to grow. Although it does not perfectly match the experimental data, it enable us to predict the stiffness of the gel network a relatively long time after salt addition.

#### 4. Discussion and conclusion

In this study, we have focused on the gelation of low volume fraction colloidal silica suspensions. We have modified the effect of interparticle force by manipulating ionic strength of the dispersion, simply by changing salt concentration in the aqueous suspending fluid. We have explored the gel time, gel structure and properties by DLS, SLS and rheological measurements. In particular, we have determined the time to gelation by each method. Accordingly, we have gained understanding on the sudden reduction of mobility as well as the divergence of relaxation time from DLS on the threshold of gelation, which coincides with a measurable elastic modulus in the rheology; the viscosity shows a dramatic increase at the gel point under weak shear. The

structure of the aggregates during the gelation process is investigated by static light scattering to determine the fractal dimension,  $D_f$ . We found  $D_f \approx 2.0$ . This fractal dimension is slightly below values found by other authors for a reaction-limited aggregation process (e.g. ref. 21), but we have demonstrated the ability to tune the aggregation rate (and hence gelation time) over orders of magnitude using the dependence of the repulsive portion of the interparticle force potential upon the ionic strength of the solvent. It is generally agreed that the RLA process provides more opportunities for particles and clusters to interpenetrate and results in more compact clusters than diffusion-limited aggregation.<sup>32</sup> However, our results finding values of the fractal dimension slightly below the value of  $D_f = 2.1$  predicted by RLA simulations suggest that the detailed form of the repulsive potential and the hydrodynamic interactions of particles must be accounted in simulation of nanoparticle gelation. Our ongoing work explores this last issue, and will be reported later.

The combination of results from both dynamic light scattering and rheology indicates that there is a universal behavior in the particle aggregation and gelation process. We found that the size, the structure, the viscosity and the elastic properties of the aggregates/gel exhibit similar behavior for a given silica volume fraction when the time is scaled as  $t/t_{gel}$ . This suggests that the salt concentration only affects the electrostatic repulsive barrier, and consequently changes the aggregation rate and the gel time. The observation that scaling by the measured gel time in RLA for silica particle gelation provides a collapse of the data both before and after the gelation for same  $\phi$  leads to the interpretation that cluster growth and gelation are composed of a set of microscopic aggregation events, which are, statistically speaking, essentially similar for different gel times. Thus the gel time may be viewed as some multiple  $N$  of a microscopic time  $t_{micro}$ , i.e.  $t_{gel} = Nt_{micro}$ , which varies with the salt concentration; the salt concentration effect is presumably due to the change in the pair interaction potential, with the 'reaction time' reduced as the repulsive part of the pair potential decreases owing to salt addition.

The microscopic time has not been probed here, but we can gain insight by noting that a similar collapse of data by Sefcik *et al.*<sup>8</sup> for the post-gelation properties only in a surfactant-stabilized polymer latex, used a scaling of time as  $t/t^*$  where  $t^* = (3\eta W)/(8kTn_0)$  is a time scale based on microscopic properties of the sol. The quantity  $W$  is termed the *stability ratio* of primary particles and captures the 'reaction' aspect of the process,  $n_0$  is the number density of primary particles in the initial sol, and other symbols have their definition used above in describing our work. The stability ratio is defined as the rate of aggregation of pairs in the pure diffusion limit to this rate under the actual conditions and is thus deduced from data on the initial growth of clusters; for RLA,  $W > 1$  and can, in fact, be very large. The number density can be written  $n_0 = 3\phi/(4\pi a^3)$ . Hence, if there is no repulsion between particles,  $W \rightarrow 1$  and this time may be written  $t^* = 4\pi\eta a^3/8kT\phi$ , showing that intrinsic rate for motion on the particle scale is given by Brownian diffusion  $t_{Br} \sim a^2/D_0 \sim \eta a^3/kT$  and increasing  $\phi$  decreases aggregation time as distances between particles are decreased. However, when there is a repulsive portion of the pair interaction, many 'attempts' are needed for a particle to cross the barrier and become a part of an aggregate, so that the microscopic timescale becomes

$$t^* (= t_{\text{micro}}) = \frac{4\pi\eta a^3 W}{8kT\phi},$$

where we now suggest that it may be appropriate to equate  $t^* = t_{\text{micro}}$  in our expression  $t_{\text{gel}} = Nt_{\text{micro}}$ .

The remarkable aspect of the collapse under this scaling is that a single time is able to satisfactorily describe the basic process for materials which are radically different in structure and properties. This collapse was limited in our work to  $\phi \leq 4\%$ , but extended to higher  $\phi$  in Ref. 8 suggesting some differences in the extent of the repulsive potential relative to the particle size (*i.e.* Debye length effects). We propose a simple gelation mechanism to help illustrate the gelation process. The transition from sol to initial gel and final gel is composed of a series of identical steps ( $t_{\text{micro}}$ ). The number of steps ( $N$ ) needed to reach initial gel or final gel state are the same for fixed  $\phi$ , independent of salt concentration. However, the height of the step varies with the salt concentration (higher salt concentration means smaller  $t_{\text{micro}}$ ). At each step ( $t = n_i t_{\text{micro}}$ ), the cluster or gel has the same structure and properties. When the time ( $t = n_i t_{\text{micro}}$ ) is scaled by the gel time ( $t_{\text{gel}} = Nt_{\text{micro}}$ ), the scaled time will be  $t/t_{\text{gel}} = n_i/N$ . The cluster or gel properties as a function of the scaled time thus are independent of the salt concentration during the gelation process. The key point is that for a fixed  $\phi$ , the gel time is a *fixed* multiple  $N(\phi)$  independent of the ionic strength. Since the dynamic data continue to be collapsed to a master curve after gelation when time is scaled by  $t_{\text{gel}}$ , we conclude that a similar microscopic timescale is operative in setting the growth rate of the network after initial gel formation. A practical benefit is that this scaling behavior enables us to predict the kinetic and mechanical properties for the gelation of colloidal silica suspensions for salt concentrations not studied.

## Acknowledgements

This work was supported in part by the US Army STTR program in cooperation with CFD Research Corporation, and in part by the NSF supported PREM at CCNY (grant DMR 0934206).

## References

1 S. Ramakrishnan, V. Gopalakrishnan and C. F. Zukoski, *Langmuir*, 2005, **21**, 9917–9925.

- 2 A. S. Zackrisson, A. Martinelli, A. Matic and J. Bergenholtz, *J. Colloid Interface Sci.*, 2006, **301**, 137–144.
- 3 J.-Z. Xue, D. J. Pine, S. T. Milner, X. L. Wu and P. M. Chaikin, *Phys. Rev. A: At., Mol., Opt. Phys.*, 1992, **46**, 6550–6563.
- 4 J. G. H. Joosten and J. L. McCarthy, *Macromolecules*, 1991, **24**, 6690–6699.
- 5 T. Coviello and W. Burchard, *Macromolecules*, 1992, **25**, 1011–1012.
- 6 S. Richter, V. Boyko, R. Matzker and K. Schröter, *Macromol. Rapid Commun.*, 2004, **25**, 1504–1509.
- 7 Y. Otsubo, *Adv. Colloid Interface Sci.*, 1994, **53**, 1–32.
- 8 J. Sefcik, R. Grass, P. Sandkühler and M. Morbidelli, *Colloids Surf., A*, 2001, **190**, 89–98.
- 9 J. So, S. Yang, C. Kim and J. C. Hyun, *Colloids Surf., A*, 2001, **190**, 89–98.
- 10 V. Trappe and P. Sandkühler, *Curr. Opin. Colloid Interface Sci.*, 2004, **8**, 494–500.
- 11 V. Prasad, V. Trappe, A. D. Dinsmore, P. N. Segre, L. Cipelletti and D. A. Weitz, *Faraday Discuss.*, 2003, **123**, 1–12.
- 12 W. Götzke and L. Sjögren, *J. Phys. C: Solid State Phys.*, 1988, **21**, 3407–3421.
- 13 W. van Meegen and S. M. Underwood, *Phys. Rev. Lett.*, 1993, **70**, 2766–2769.
- 14 D. R. Reichman and P. Charbonneau, *J. of Stat. Mech.: Theory and Experiments*, 2005, 05013.
- 15 C. Beck, W. Härtl and R. Hempelmann, *J. Chem. Phys.*, 1999, **111**, 8209–8213.
- 16 H. E. Bergna, *Phys. Rev. Lett.*, 1986, **57**, 3117.
- 17 D. W. Schaefer and J. E. Martin, *Phys. Rev. Lett.*, 1984, **52**, 2371–2374.
- 18 J. E. Martin, *Phys. Rev. A: At., Mol., Opt. Phys.*, 1987, **36**, 3415–3426.
- 19 C. Aubert and D. S. Cannell, *Phys. Rev. Lett.*, 1986, **56**, 738–741.
- 20 W. Shih, W. Y. Shih, S. Kim, J. Liu and I. A. Aksay, *Phys. Rev. A: At., Mol., Opt. Phys.*, 1990, **42**, 4772–4779.
- 21 M. Y. Lin, H. M. Lindsay, D. A. Weitz, R. C. Ball, R. Klein and P. Meakin, *Phys. Rev. A: At., Mol., Opt. Phys.*, 1990, **41**, 2005–2020.
- 22 C. J. Rueb and C. F. Zukoski, *J. Rheol.*, 1997, **41**, 197–217.
- 23 H. J. M. Hanley, C. D. Muzny, B. D. Butler, G. C. Straty, J. Bartlett and E. Drabarek, *J. Phys.: Condens. Matter*, 1999, **11**, 1369–1380.
- 24 A. H. Krall and D. A. Weitz, *Phys. Rev. Lett.*, 1998, **80**, 778–781.
- 25 T. Matsunaga and M. Shibayama, *Phys. Rev. E: Stat., Nonlinear, Soft Matter Phys.*, 2007, **76**, 030401.
- 26 G. Dietler, C. Aubert and D. S. Cannell, *Colloidal Silica: Fundamentals and Applications*, 2006, 9.
- 27 *Principles of Polymer Chemistry*, ed. P. J. Flory, Cornell Univ. Press, 1953.
- 28 J. A. Lewis, *J. Am. Ceram. Soc.*, 2004, **83**, 2341.
- 29 H. H. Winter and F. Chambon, *J. Rheol.*, 1987, **31**, 683–697.
- 30 E. Drabarek, J. Bartlett, H. J. M. Hanley, J. L. Woolfrey and C. D. Muzny, *Int. J. Thermophys.*, 2002, **23**, 145.
- 31 J. W. Jansen, C. de Kruif and A. Vrij, *J. Colloid Interface Sci.*, 1986, **114**, 481–491.
- 32 M. Jokinen, E. Györvary and J. B. Rosenholm, *Colloids Surf., A*, 1998, **141**, 205–216.